Effect of a Ti diffusion barrier on the cobalt silicide formation: solid solution, segregation and reactive diffusion

Hannes Zschiesche, Claude Alfonso, Ahmed Charaï, Dominique Mangelinck

Effect of a Ti diffusion barrier on the cobalt silicide formation: solid solution, segregation and reactive diffusion

Hannes Zschiesche[a,b,*], Claude Alfonso[a], Ahmed Charaï[a], Dominique Mangelinck[a]

[a] *CNRS, IM2NP, Aix-Marseille Université, Service 142, Faculté de Saint-Jérôme, 13397 Marseille Cedex 20, France.*
[b] *McMaster University, Department of Materials Science and Engineering, 1280 Main Street West Hamilton, ON L8S 4L8, Canada.*

Abstract

Diffusion barriers play an important role in numerous phase formation processes. A well known example in microelectronics is the reactive diffusion growth of silicide thin films which are applied as contact materials. In this work, the effect of a Ti interlayer on the kinetics of the formation of CoSi by reactive diffusion is investigated. Therefore, Co(100 nm)/Ti(5 nm) deposited on Si(111) is annealed at various temperatures. Transmission electron microscopy and atom probe tomography allow to study the evolution of microstructure and local compositions after each annealing. It is observed that the CoSi growth starts at the Ti/Si interface and it is controlled by Co diffusion through the Ti interlayer. The Ti interlayer keeps its microstructure during the growth of CoSi. At higher annealing temperatures, Si diffusion through the Ti interlayer to the Co layer is evidenced. First, it segregates at grain boundaries of the polycrystalline Co layer on top of the Ti interlayer before it reacts to cobalt silicides. Also Ti diffusion to the CoSi/Si interface occurs that may affect diffusion processes and phase formation reaction at this interface. Beyond the experimental observations, a model is developed to quantify the diffusivity of Co in the Ti interlayer on the base of the investigated CoSi growth. Furthermore, a model is developed in order to estimate the diffusivity of Si in the Ti interlayer on the base of the formed solid solution and segregation in the Co layer. Both models can be generally applied for similar material configurations to estimate diffusivities in interlayers or to predict phase growth.

*Corresponding author: Hannes Zschiesche; *email:* hannes.zschiesche@mpikg.mpg.de; *Tel.:* +49 (331) 567-9513; *Current address:* Max Planck Institute of Colloids and Interfaces, Am Muehlenberg 1, 14476 Potsdam, Germany

Keywords: diffusion barrier, reactive diffusion, segregation, transmission electron microscopy, atom probe tomography

1. Introduction

Silicides like $TiSi_2$, $CoSi_2$ and NiSi are widely used in microelectronics as contact material in form of thin films [1]. The properties of these thin films depend strongly on their microstructure and local chemistry. These are influenced by the phase formation process. Understanding and controlling the phase formation process is thus crucial for the quality of thin films and more general for any kind of formed material.

In a layered system, phase formation occurs often by reactive diffusion in which interface reactions and diffusion contribute [2, 3, 4, 5]. After nucleation of a phase at an interface, usually a lateral growth occurs until a layer is formed prior perpendicular thickness growth of this layer [6, 7]. The growth comprises the process of the rearrangement of atoms at the interface of the growing phase and the diffusion of matter which is needed to form units of the growing phase. The perpendicular thickness growth rate can be limited either by the diffusion of matter through the forming layer, so called diffusion controlled, or by the reactivity at an interface, so called interface controlled (or reaction controlled). Generally, sequential formation of phases with possible absence of some equilibrium phases is observed in thin films [8] (typically between 10 and 200 nm [9]) while growth of all equilibrium phases takes place in bulk simultaneously [10].

One possibility to control phase formations by reactive diffusion is the introduction of an interlayer between the reacting materials. An interlayer can be either introduced during materials growth (deposition) or arose from segregation and/or redistribution of alloying elements or impurities contained in one of the materials. An interlayer acts as diffusion barrier when it separates the reacting materials with a restricted diffusivity of the reacting materials [11]. In addition, the interlayer material may affect nucleation involved in the phase formation process by changing Gibbs volume energy terms when it is soluble in one of the phases involved in the reaction [12] or by changing interface energy terms when it segregates at interfaces [13]. Influencing the phase formation by an interlayer is not only interesting for con-

tacts and interconnections in microelectronics, but also for many other engineering applications like protective coating in metallurgy [14], interlayer in diffusion welding [15] or intermetallic control in aeronautics [16, 17].

Co thin film reaction with silicon can be seen as a model system for reactive diffusion and presents a large interest for applications. $CoSi_2$ is the phase in the Co-Si binary system that attracts the most attention for applications because of its high electrical conductivity, thermal stability and good match of the crystal structure with Si [1]. $CoSi_2$ thin films can be obtained by thermal annealing of pure Co on Si that leads to a sequential formation of the equilibrium phases Co_2Si, CoSi and $CoSi_2$ [18, 19].

Epitaxial $CoSi_2$ thin films are reported when molecular beam epitaxy (MBE) was used [20, 21], in agreement with the expectations from the small lattice mismatch, while textured polycrystalline $CoSi_2$ thin films are known to form from reactions of Si substrate and Co layers deposited by sputtering [22]. Reasons for the polycrystalline $CoSi_2$ thin film when using sputtering can be the introduction of contaminants due to lower purity in the vacuum of the sputtering chamber, the sputtering gas or limited possibilities to clean the substrate surface without contact to air prior deposition. In consequence, the formation of $CoSi_2$ at the Co/Si interface is impeded by the presence of native oxide which is formed either prior the deposition process or by reaction of oxygen contamination in the deposited Co layer with Si substrate. $CoSi_2$ microstructures close to the ones grown by MBE are obtained from sputtered deposition when a thin Ti interlayer is introduced between Si and Co for the sputtering process and even epitaxial $CoSi_2$ thin films with similar quality as the one obtained by MBE have been reported [23, 24]. This is known as Ti interlayer mediated epitaxy (TIME). In addition to the initial idea that the Ti interlayer removes native oxides at the Si interface, a shift of the cobalt silicides formation completion to higher temperatures was observed which causes a lower sensitivity for cobalt silicide formations on oxides [25].

Other materials than Ti have been studied as interlayers in the formation of $CoSi_2$ [26, 27, 28, 29]. One of the most prominent might be a Si oxide interlayer which is reported to lead as well to an increase of epitaxially orientated $CoSi_2$ grains, known as oxide mediated epitaxy [30]. This example of expansive application of reactive

diffusion growth through interlayers shows the demand for models which describe the phase formation by diffusion and reaction. Recently, a model was developed describing reactive diffusion in the presence of an interlayer [11]. Therein, Ni silicide formation was investigated under the influence of two types of barriers: (i) a thin layer of W deposited between a Ni film and Si substrate and (ii) Ni alloy films, Ni(1% W) and Ni(5% Pt), that form a diffusion barrier during the reaction with the Si substrate. For the δ-Ni_2Si formation by reactive diffusion, the main diffusing species (higher mobility in growing phase in comparison with other involved elements) is the metal Ni [31] and δ-Ni_2Si is expected to grow at the Si rich interface (δ-Ni_2Si/Si). The developed model considers therefore the reactive diffusion in the presence of a diffusion barrier when the main diffusing element in the growing phase is also the element which diffuses through the diffusion barrier.

Two experimental techniques which provide local information on samples are (scanning) transmission electron microscopy ((S)TEM) [32] and atom probe tomography (APT) [33, 34]. (S)TEM gives structural (imaging) and analytic (energy dispersive X-ray spectroscopy (EDS)) information with spatial resolution down to sub-Å distance. APT enables the reconstruction of a 3D volume with sensitivity to single atoms and spatial resolutions down to crystal lattice plane distances. An analysis of phase formation and growth at various annealing temperatures is possible using both techniques on samples after each annealing temperature.

In our work, the effect of the Ti interlayer on the reactive diffusion growth of CoSi is investigated. Using atomic scale investigations such as APT with complementary (S)TEM imaging and EDS analysis gives new insights in the formation of cobalt silicides in the presence of a a Ti interlayer as well as the evolution and role of the Ti interlayer. In particular, the following points have been addressed: i) Probing the thermal stability of the Ti interlayer. ii) Investigating the diffusion, phase formation and growth in the Co/Ti/Si configuration. iii) Developing models for the diffusion in the presence of a diffusion barrier to describe our observations in ii) and i). iv) Applying the models in order to determine Co and Si diffusivities in the Ti interlayer.

2. Experimental

Co/Ti/Si as-deposited bilayer samples were grown using magnetron sputtering. Before load into the sputtering system, parts of Si(111) wafers were immersed in a 5 % dilute HF for 1 min to remove native oxide. Successive deposition of 5 nm Ti and 100 nm Co from two individual targets of Ti and Co (both 99.99 % purity) was done. The deposition was performed with a base pressure of about 10^{-8} Torr using 99.9999 % pure Ar and a gas flow of 6.7 sccm at room temperature. Isothermal annealing were performed in vacuum successively at 400 °C, 500 °C, 550 °C and 570 °C each for 10 min in order to activate diffusion and phase formation.

(S)TEM cross-section imaging, EDS-STEM analysis and APT were performed on the as-deposited and the annealed samples. TEM lamella and APT tips were prepared using a focused ion beam (FIB) `FEI Helios 600` with a Ga^+ source following common procedures for TEM lamella [35] and APT tips [36]. (S)TEM measurements were done on a `FEI TECNAI G20` using 200kV. EDS-STEM was performed using an `EDS SDD Oxford XMax80` detector equipped with `AZtec` software. APT measurements were performed on a `LEAP 3000X HR`. Voltage mode at 40 K, 200 kHz, 20 % pulse fraction and 0.2 % detection rate was applied. `IVAS` software was used for the reconstruction [37, 38]. Either information from complementary (S)TEM imaging (layer thicknesses) or crystallographic information in the APT volume (crystal lattice plane distances in identified pole [39]) were used to adjust the reconstruction parameters. Simulations on the base of the experimental results were run in `Matlab`.

3. Results

3.1. Phase formation and growth visualized in (S)TEM

Fig. 1 shows bright field (BF) (S)TEM images of the as-deposited bilayer (Fig. 1a), after annealing at 500 °C (Fig. 1b), 550 °C (Fig. 1c) and 570 °C (Fig. 1d) in cross-section. The images are visualized at identical scale. Note that the Si substrate on the right of the images appears in darker contrast due to zone axis orientation that enables a viewing direction in parallel to the initial substrate interface. In combination with related EDS-STEM line scans perpendicular to the substrate interface (Fig. 1e to 1h), as-deposited microstructure and diffusion and phase formation at the

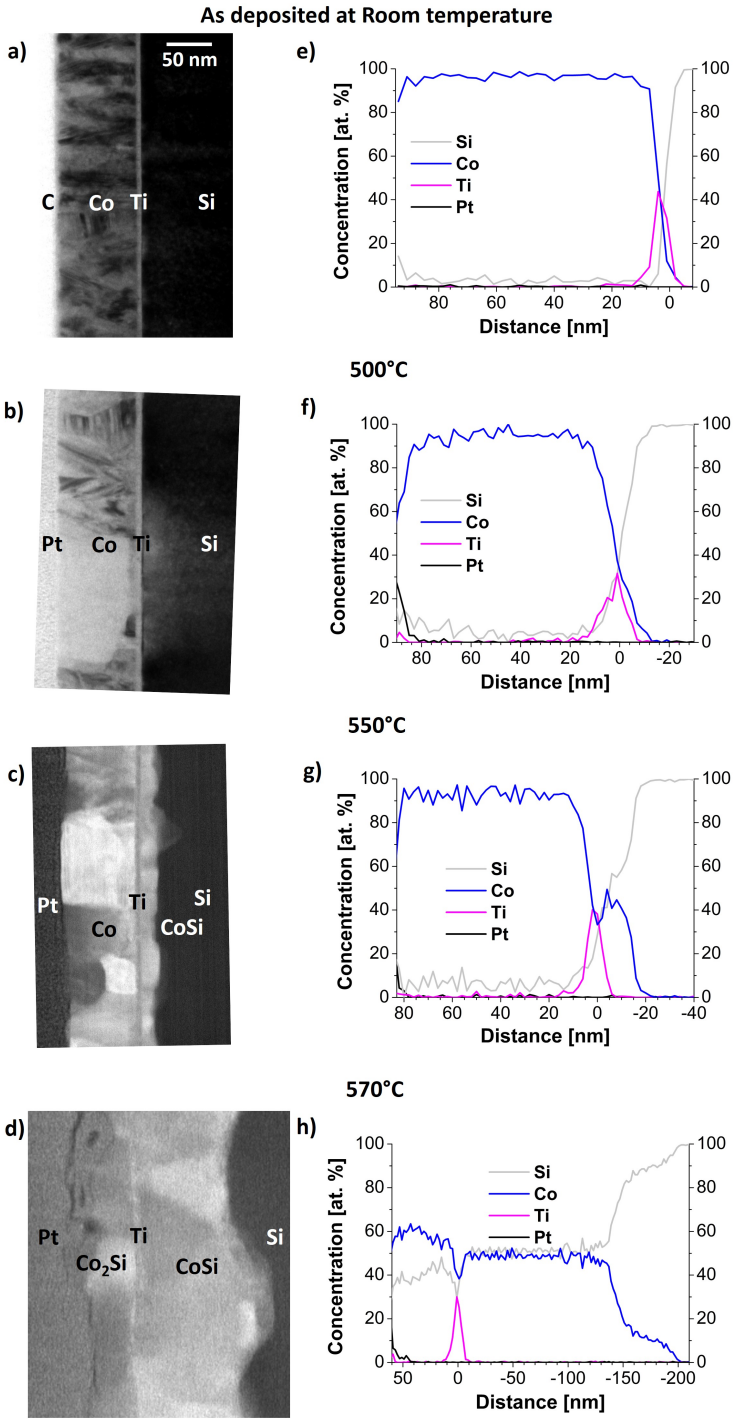

Figure 1: (a)-(d) BF (S)TEM cross-section images of as-deposited, annealed at 500 °C, 550 °C and 570 °C, respectively. (e)-(h) According EDS-STEM line-scans crossing the substrate interface perpendicular. Note that the scale of the (S)TEM images is identical while the scale for the EDS-STEM line-scans varies.

annealing temperatures can be interpreted as follows. The Ti and the Co deposited at room temperature form homogeneous polycrystalline layers of about 5 nm and

100 nm, respectively. The Ti interlayer separates spatially Co and Si and it can act as a diffusion barrier during initial silicide formation. C and Pt were post-deposited on the thin film sample during TEM lamella preparation and have no influence on the investigated diffusion and phase formation. The Si signal inside the Co layer of Fig. 1e to 1g is not attributed to Si atoms within the Co layer, but generated in the Si substrate by fluorescence radiation (Co K-edge 7.71 keV, Ti K-edge 4.97 keV, Si K-edge 1.84 keV) or within another part in the microscope (sample holder, pole piece, etc.).

After annealing at 500 °C, Co has diffused through the Ti interlayer and started to react with the Si substrate (Fig. 1b and 1f). The Ti interlayer itself is still visible in the TEM observation as a homogeneous layer and thus, the microstructure of the Ti interlayer is stable at this temperature and under Co diffusion from the Co layer to the Si substrate. After further annealing at 550 °C for 10 min, a CoSi layer of about 15 nm has formed between the homogeneous Ti interlayer and the Si substrate (Fig. 1c and Fig. 1g). In contrast, no cobalt silicide is formed simultaneously at the Co/Ti interface. The CoSi layer between Si substrate and Ti interlayer continues growing to a thickness of about 140 nm during annealing at 570 °C for further 10 min. The Ti interlayer is present, but its planar shape adjusts to the microstructure of the CoSi layer that is growing between the Ti interlayer and the Si substrate. Additionally, formation of Co_2Si occurred in the Co layer on top of the Ti interlayer. Thus, Si must have diffused from the substrate through the growing CoSi layer and the Ti interlayer towards the Co. To get generally 3D information with higher elemental sensitivity at atomic scale in all deposited layers and the growing phase, complementary APT analysis were performed on the samples after various annealing and selected results are presented now.

3.2. 3D APT analysis on diffusion and segregation

Fig. 2 shows APT results of investigations on the early stage Co diffusion inside the Ti interlayer. A reconstruction of an acquired APT volume of a sample annealed at 400 °C is visualized in Fig. 2a. The Ti interlayer is flat with a thickness of about 5 nm as observed in (S)TEM imaging. A 1D concentration profile is given in Fig. 2b based on a proxigram analysis [40] using a 40 at % Ti surface close to the Si substrate.

The profile verifies that Co has not diffused through the entire Ti interlayer. In addition, information about the chemistry in the Ti interlayer is revealed. Fig. 2b shows that C and O, which are known as contaminants of the sputtering deposition process, are enriched in the Ti interlayer. While the C concentration (up to 20 at %) is distributed over the entire Ti interlayer, the O concentration is higher (up to 5 at %) close to the Ti/Si interface. The concentrations of C and O are much lower in the Co layer.

A similar APT analysis for a sample after annealing at 500 °C is given in Fig. 2c and 2d. As shown in the (S)TEM investigations (Fig. 1f), Co has diffused through the entire Ti interlayer and forms a thin CoSi layer of about 3 nm (blue arrow in Fig. 2c and 2d). The width of and the composition in the Ti interlayer are approximately the same as for the sample annealed at 400 °C. Differences are the higher Co concentration close to the Si substrate and a Si concentration at the Co/Ti interface of almost 10 at %.

In Fig. 3, an APT analysis of a sample after annealing at 550 °C is presented.

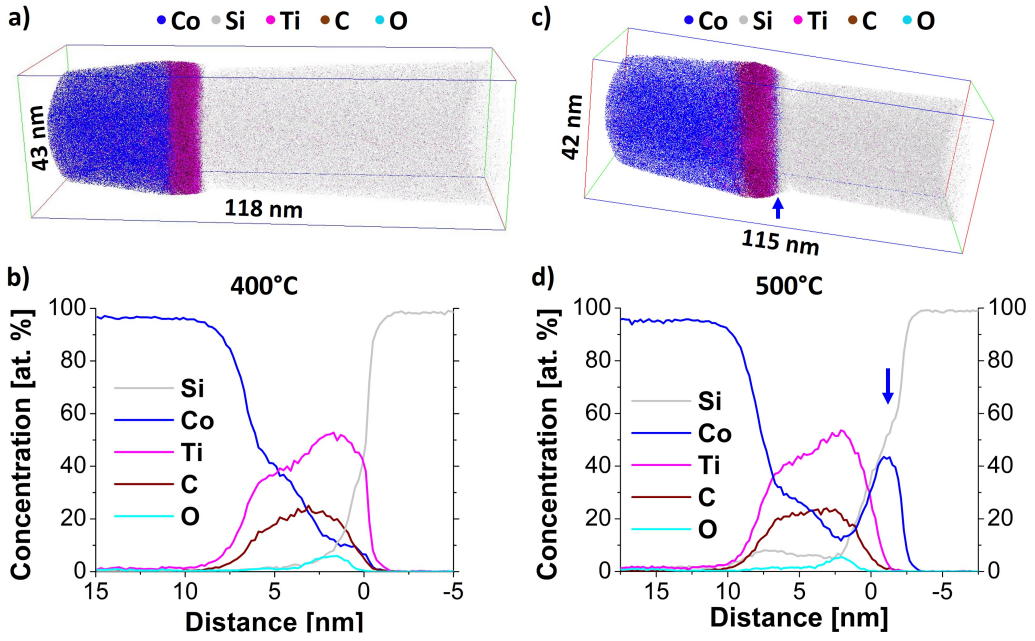

Figure 2: APT analysis in the proximity of the Ti interlayer. a) and c) reconstructions of 3D volumes. b) and d) Proxigrams of a 40 at % Ti surface close to the Si substrate. While Co has not diffused through the entire Ti interlayer after annealing at 400 °C for 10 min (a) and b)), it starts to form CoSi at the Ti/Si interface after annealing at 500 °C for 10 min (blue arrow in c) and d)).

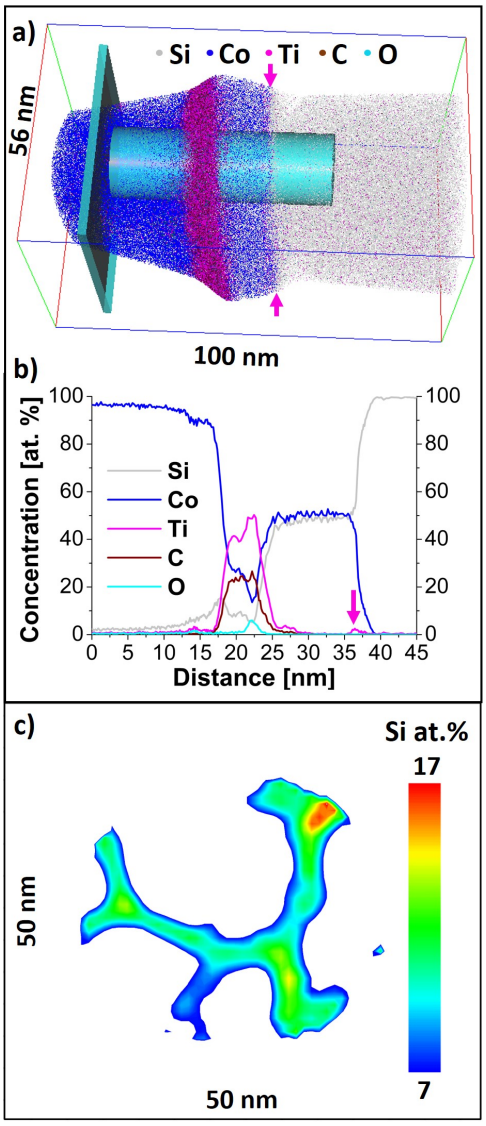

Figure 3: APT analysis after annealing at 550 °C. a) Reconstructed volume including a cylinder for a 1D concentration profile presented in b) which cross the CoSi/Si interface and the Ti interlayer approximately perpendicular, and a slice for a 2D Si concentration map shown in c). CoSi has grown, Ti segregates at the CoSi/Si interface and Si segregates at Co grain boundaries in the deposited top layer during the annealing.

Fig. 3a visualizes the reconstructed volume. The reconstruction parameters were chosen to get a flat homogeneous Ti interlayer as observed in the TEM investigation (compare Fig. 1c). The shown cylinder inside the volume was used for a 1D concentration profile which crosses the CoSi/Si interface and Ti interlayer approximately perpendicular. In this profile (Fig. 3b), the cross-section composition of Ti interlayer is the same as the one observed after annealing at 500 °C (compare to

Fig. 2d). This implies that the Ti interlayer does not change its composition even if further Co diffusion takes place ensuring the growth of the CoSi layer. Furthermore, Ti segregation is found at the CoSi/Si interface (magenta arrows in Fig. 3a and 3b). In addition, a further increase of the Si concentration at the Co/Ti interface is observed up to 15 at % and the Si concentration inside the Co layer is not negligible: a monotone decrease from the Co/Ti interface towards the sample surface is observed. A visualization of the lateral Si distribution inside the Co layer is given in Fig. 3c as a 2D Si concentration map projected along the short side of the slice inside the Co layer (see slice in Fig. 3a). The visualized Si concentration ranges from 7 at% to 17 at %. The Si distribution is inhomogeneous and this is interpreted as Si segregation at Co grain boundaries. It implies that Si diffuses through the Ti interlayer into the Co layer to form cobalt silicides at higher annealing temperatures as observed in (S)TEM (Fig. 1d and 1h).

The divers results of (S)TEM and APT investigation will now be discussed and used to develop a model for a description of the observed diffusion.

4. Discussion

In literature about CoSi thin film growth, it was shown that Si diffuses faster than Co in CoSi for reactive diffusion in a Co_2Si/CoSi/Si configuration without Ti interlayer [19]. Thus, the CoSi growth is controlled by Si diffusion through the CoSi layer when the interface reactivity is sufficiently fast in comparison to the Si permeability in CoSi [19]. In our sample, the configuration for the CoSi growth is changed due to the presence of a Ti interlayer between Co layer and the Si substrate. The Ti interlayer acts as a diffusion barrier between the Co source and the Si substrate (Fig. 1). It results that the formation of Co_2Si at the Si substrate interface is skipped (in agreement with literature [41]) and CoSi forms directly at the Ti/Si interface. Thereby, the configuration for the CoSi growth at the Ti/Si interface by reactive diffusion is changed to Co/Ti/CoSi/Si in which Co diffuses through the Ti interlayer and controls the CoSi growth rate. Modeling this reactive diffusion configuration should permit to determine the Co diffusivity in the Ti interlayer.

4.1. Reactive diffusion in the presence of an interlayer

In order to determine the diffusivity of an interlayer, the growth of one phase (η) with a barrier (β) when B diffuses faster than A in η was modeled and is schematized in Fig. 4. It is therefore assumed that the diffusion, and not the interface reactivity, controls the phase growth. Recently, an approach when A diffuses faster than B in η was developed by Mangelinck et al. [11]. This approach does not cover the case in which the main diffusing element in the growing phase does not diffuse through the diffusion barrier for the phase growth. For example the CoSi formation in the Co/Ti/Si configuration: Si is the main diffusing element in the formation of CoSi [19, 42] and it is shown that CoSi nucleates at the Ti/Si interface (Fig. 1) and the perpendicular growth takes place at the Ti/CoSi interface so that Co has to diffuse through the Ti diffusion barrier while Si does not. Thus, a model for reactive diffusion in the presence of a diffusion barrier needs to be developed in which the diffusion of two elements is considered.

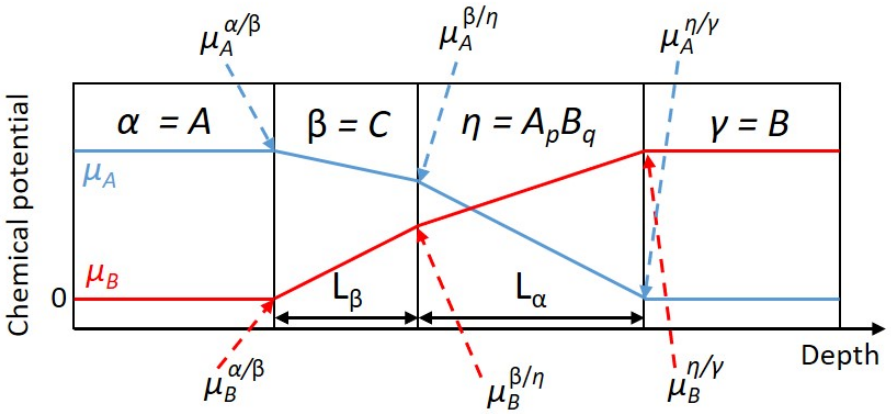

Figure 4: Schematic of the growth of a phase $\eta = A_pB_q$ (CoSi) rate limited by diffusion of A (Co) atoms through a barrier β (Ti interlayer).

In accordance to the Co/Ti/Si sample the labeling was chosen α = Co, β = Ti interlayer, η = CoSi and γ = Si with A = Co and B = Si. The growth of the phase η at the interface to the barrier (β/η) can be described by the flux J_B^η of the mobile species B in η and the formed volume $\Omega^\eta_{\beta/\eta,B}$

$$\frac{dL^\eta}{dt} = \Omega^\eta_{\beta/\eta,B} J_B^\eta. \quad (1)$$

In analogy, it can be described by the flux J_A^β of A atoms in β. In both cases, dL^η describes the increase in thickness of η per time unit dt. The formed volume of η by atom of the mobile species B in η can be further described by

$$\Omega^\eta_{\beta/\eta,B} = \frac{1}{q}\Omega^\eta_B = \frac{p+q}{q}\,\omega^\eta_B = \frac{\omega^\eta_B}{x^\eta_B} = \frac{1}{c^\eta_B}. \quad (2)$$

Where Ω^η, ω^η, x^η_B and c^η_B are, respectively, the volume occupied by a formula unit, the atomic volume, the atomic fraction and the concentration of the diffusing species ($B \to A$ in analogy). It permits to rewrite Eq. 1

$$\frac{dL^\eta}{dt} = \Omega^\eta_{\beta/\eta,B} J^\eta_B = \frac{1}{c^\eta_B} J^\eta_B. \quad (3)$$

It is appropriate to consider diffusion in terms of the modified Nernst-Einstein equation

$$J^\eta_B = -c^\eta_B \left(\frac{D^\eta_B}{k_B T}\right) \frac{\partial \mu^\eta_B}{\partial z} \quad (4)$$

$$J^\beta_A = -c^\beta_A \left(\frac{D^\beta_A}{k_B T}\right) \frac{\partial \mu^\beta_A}{\partial z}. \quad (5)$$

Furthermore, $\partial\mu^\eta_B/\partial z$, the gradient of chemical potential is taken equal to $\Delta\mu^\eta_B/L^\eta$ with $\Delta\mu^\eta_B$, the absolute chemical potential change per moving atom B ($\Delta\mu^\eta_B = |\mu^{\beta/\eta}_B - \mu^{\eta/\gamma}_B|$):

$$J^\eta_B = c^\eta_B \left(\frac{D^\eta_B}{k_B T}\right) \frac{\Delta\mu^\eta_B}{L^\eta}. \quad (6)$$

In analogy, it follows for the flux of A through β that $\partial\mu^\beta_A/\partial z$ is taken equal to $\Delta\mu^\beta_A/L^\beta$, with $\Delta\mu^\beta_A$, the absolute value of the chemical potential change per moving A atom ($\Delta\mu^\beta_A = \left|\mu^{\beta/\eta}_A - \mu^{\alpha/\beta}_A\right|$):

$$J^\beta_A = c^\beta_A \left(\frac{D^\beta_A}{k_B T}\right) \frac{\Delta\mu^\beta_A}{L^\beta}. \quad (7)$$

In order to form a unit of A_pB_q, p atoms of A have to combine with q atoms of B. Thus for the formation of a A_pB_q unit, the flux of A crossing the barrier (β) and the flux of B crossing the growing phase (η) should verify the following relationship at the β/η interface:

$$qJ^\beta_A = pJ^\eta_B \quad (8)$$

$$q \cdot c_A^\beta \left(\frac{D_A^\beta}{k_B T}\right) \frac{\Delta\mu_A^\beta}{L^\beta} \quad = \quad p \cdot c_B^\eta \left(\frac{D_B^\eta}{k_B T}\right) \frac{\Delta\mu_B^\eta}{L^\eta} \tag{9}$$

In the following, we will consider that the interfaces are at local equilibrium and thus that the chemical potentials are equal on each side of the interface. If the end members (α and γ) are considered as pure elements (A and B), the chemical potentials $\mu_A^{\alpha/\beta}$ and $\mu_B^{\eta/\gamma}$ are null and the variation of the chemical potentials across β and η are given by:

$$\Delta\mu_A^\beta \quad = \quad \left|\mu_A^{\beta/\eta}\right| \tag{10}$$

$$\Delta\mu_B^\eta \quad = \quad \left|\mu_B^{\beta/\eta}\right| \tag{11}$$

Furthermore, if the η phase is stoichiometric the chemical potential of A and B are related to the absolute value of Gibbs energy of formation of the phase per mole of atoms G^η:

$$-G^\eta \quad = \quad \frac{p}{p+q}\mu_A^\eta + \frac{q}{p+q}\mu_B^\eta \tag{12}$$

Eq. 12 is valid anywhere inside η and thus also at the β/η interface:

$$\mu_A^{\beta/\eta} \quad = \quad -\frac{(p+q)}{p}G^\eta - \frac{q}{p}\mu_B^{\beta/\eta} \tag{13}$$

Eq. 9 can be rearranged using Eq. 13

$$\mu_B^{\beta/\eta} \quad = \quad \frac{p+q}{q}\, G^\eta\, \frac{1}{1+\dfrac{p^2}{q^2}\dfrac{c_B^\eta}{c_A^\beta}\dfrac{L^\beta}{L^\eta}\dfrac{D_B^\eta}{D_A^\beta}} \tag{14}$$

Note that the term, $\frac{p+q}{q}G^\eta$, corresponds to the variation of chemical potential of B across the η phase when η is growing between pure A and pure B without barrier, $\Delta\mu_B^{\eta,nb}$. If the diffusion of B in η is very fast, the chemical potential of B at the β/η interface is close to zero (i.e. Eq. 14 with $D_A^\beta \ll D_B^\eta$) as it should be in pure B (or in γ with very limited solubility of A). Applying this approximation

to Eq. 13, the chemical potential of A at the β/η interface is equal to $\frac{p+q}{p}G^{\eta}$ and thus:

$$\Delta\mu_A^{\beta} \approx \Delta\mu_A^{\eta,nb} \approx \frac{p+q}{p}G^{\eta} \tag{15}$$

Eq. 15 means that all the gradient of chemical potential is across the barrier. With Eq. 14, Eq. 3 can be rewritten to

$$\frac{dL^{\eta}}{dt} = \frac{1}{c_B^{\eta}}J_B^{\eta} \tag{3}$$

$$\frac{dL^{\eta}}{dt} = \left(\frac{D_B^{\eta}}{k_BTL^{\eta}}\right)\frac{p+q}{q}G^{\eta}\frac{1}{\left(1+\frac{p^2}{q^2}\frac{c_B^{\eta}}{c_A^{\beta}}\frac{L^{\beta}}{L^{\eta}}\frac{D_B^{\eta}}{D_A^{\beta}}\right)} \tag{16}$$

$$\frac{dL^{\eta}}{dt} = \frac{p+q}{q}\frac{G^{\eta}}{k_BT}\frac{1}{\frac{L^{\eta}}{D_B^{\eta}}+\frac{p^2}{q^2}\frac{c_B^{\eta}}{c_A^{\beta}}\frac{L^{\beta}}{D_A^{\beta}}} = \frac{\Delta\mu_B^{\eta,nb}}{k_BT}\frac{1}{\frac{L^{\eta}}{D_B^{\eta}}+\frac{p^2}{q^2}\frac{c_B^{\eta}}{c_A^{\beta}}\frac{L^{\beta}}{D_A^{\beta}}} \tag{17}$$

The growth of the phase η is controlled by the lowest diffusion: either the diffusion of A through the barrier β or the diffusion of B through the growing phase η. Eq. 17 shows that the growth of the phase η is controlled by the lowest diffusion: either the diffusion of A through the barrier β or the diffusion of B through the growing phase η. If $D_A^{\beta} \gg D_B^{\eta}$, Eq. 17 becomes:

$$\frac{dL^{\eta}}{dt} = \frac{\Delta\mu_B^{\eta,nb}}{k_BT}\frac{D_B^{\eta}}{L^{\eta}}. \tag{18}$$

This represents the case when A diffuses much faster through the interlayer (β) than B through the growing layer (η). Thus, the interlayer does effectively not act as a diffusion barrier for A. Indeed, Eq. 18 represents the growth of η when only the flux of B through η is limiting. The growth of the layer η is thereby inversely proportional to its present thickness. This corresponds to the case without diffusion barrier [11].

Inversely, when the flux of A through β is much lower than the flux of B through η ($D_A^{\beta} \ll D_B^{\eta}$), Eq. 17 becomes:

$$\frac{dL^\eta}{dt} = \frac{\Delta\mu_B^{\eta,nb}}{k_BT}\frac{q^2}{p^2}\frac{c_A^\beta D_A^\beta}{c_B^\eta L^\beta}. \quad (19)$$

Using Eq. 2, Eq. 19 becomes:

$$\frac{dL^\eta}{dt} = \frac{G^\eta}{k_BT}\frac{\omega^\eta}{\omega^\beta}\frac{x_A^\beta}{(x_A^\eta)^2}\frac{D_A^\beta}{L^\beta}. \quad (20)$$

Since the terms on the right of Eq. 20 are independent of time for an isothermal heat treatment, the thickness can be expressed as:

$$L^\eta = \frac{G^\eta}{k_BT}\frac{\omega^\eta}{\omega^\beta}\frac{x_A^\beta}{(x_A^\eta)^2}\frac{D_A^\beta}{L^\beta}\Delta t = \frac{G^\eta}{k_BT}\frac{\omega^\eta}{\omega^\beta}\frac{1}{(x_A^\eta)^2}\frac{P_A^\beta}{L^\beta}\Delta t \quad (21)$$

Where Δt is the duration of the heat treatment. In this situation, the interlayer β does act as a diffusion barrier for A and the growth of η is controlled by the diffusion of A through the diffusion barrier. Thus, the thickness of the growing layer η does not influence the growth rate. The growth is linear for an isothermal annealing and depends, besides the controlling permeability ($P_A^\beta = x_A^\beta D_A^\beta$), on the inverse thickness of the interlayer, L^β, and on the driving force for the formation of the η phase, G^η.

4.2. Diffusion in the presence of an interlayer driven by segregation or the formation of a solid solution

In the preceding paragraph, the diffusion of Co (= A) through the β barrier to form CoSi was considered. The diffusion of Si (= B) through the barrier will now be examined. In a first time, this diffusion occurs to form the solid solution, α, of Co and Si and then to form Co_2Si (δ). Diffusion through an interlayer can thus occurs when B is soluble in the phase α (Fig. 4) since this will lead to a decrease of the Gibbs energy of the total system. In this case, the diffused matter is not determined from a growing phase, but by a measurement of the concentration of B in α. Indeed, an integration of the concentration of B in α measured after a time Δt corresponds to the flux of B through β:

$$\int_{\alpha} c_{\mathrm{B}}^{\alpha}\, dz \quad = \quad \int_{0}^{t} J_{\mathrm{B}}^{\beta}\, dt. \tag{22}$$

Similarly to Eq. 5, the flux J_B^β can be written as:

$$J_B^\beta \quad = \quad -\, c_B^\beta \frac{D_B^\beta}{L^\beta} \frac{\Delta\mu_B^\beta}{k_B T} \tag{23}$$

Similarly to Eq. 15, we will assume that all the gradient of chemical potential is across the barrier and thus that:

$$\Delta\mu_B^\beta \quad \approx \quad \Delta\mu_B^{\eta,nb} \quad \approx \quad \frac{p+q}{q} G^\eta \tag{24}$$

This implies that the diffusion of B from γ to α is only limited by the diffusion in the barrier β since the diffusion of B in η is very fast. Note that the chemical potential of B at the α/β interface is taken as the one corresponding to the binary equilibrium between α and η, even if the presence of Ti may modify this equilibrium.

Under these assumptions, the flux is independent of time and the right term in Eq. 22 simplifies to the product $J_B^\beta \Delta t$. Combining Eq. 22, 23 and 24, the diffusivity of B in β can be written as:

$$D_B^\beta \quad = \quad \frac{1}{\Delta t} \frac{L^\beta}{c_B^\beta} \frac{k_B T}{\Delta\mu_B^{\eta,nb}} \int_\alpha c_B^\alpha dz \tag{25}$$

A transformation to atomic fraction (x_B) from the concentration in Eq. 25 gives:

$$D_B^\beta \quad = \quad \frac{1}{\Delta t} \frac{L^\beta}{x_B^\beta} \frac{\omega^\beta}{\omega^\alpha} \frac{k_B T}{\Delta\mu_B^{\eta,nb}} \int_\alpha x_B^\alpha dz \tag{26}$$

The approximated diffusivity of A in the barrier can thus be obtained through the integration of the profile in the α phase. This determination of a diffusivity through a barrier is not only applicable for a diffusion to the formation of a solution as described above, but it can also be used in the case of reactive diffusion (i.e. formation of a new phase). Indeed, if Eq. 22 is transposed to the growth of η (c.f. Sec. 4.1) that is limited by the diffusion of A through β, one gets:

$$\int_{\eta} c_{\mathrm{A}}^{\eta}\, dz \quad = \quad \int_{0}^{t} J_{\mathrm{A}}^{\beta}\, dt. \tag{27}$$

Since c_A^η is constant, Eq. 27 can be integrated:

$$L^\eta \quad = \quad \frac{G^\eta}{k_B T}\frac{\omega^\eta}{\omega^\beta}\frac{x_A^\beta}{\left(x_A^\eta\right)^2}\frac{D_A^\beta}{L^\beta}\Delta t \quad = \quad \frac{G^\eta}{k_B T}\frac{\omega^\eta}{\omega^\beta}\frac{1}{\left(x_A^\eta\right)^2}\frac{P_A^\beta}{L^\beta}\Delta t \tag{21}$$

This is Eq. 21 and thus the two approach are equivalent within the used assumptions. The diffusion coefficient of A in the barrier β can thus be obtained by:

$$D_A^\beta \quad = \quad \frac{L^\eta L^\beta}{\Delta t}\frac{c_B^\eta}{c_A^\beta}\frac{k_B T}{\Delta\mu_A^{\eta,nb}} \tag{28}$$

$$D_A^\beta \quad = \quad \frac{L^\eta L^\beta}{\Delta t}\frac{\omega^\beta}{\omega^\eta}\frac{\left(x_A^\eta\right)^2}{x_A^\beta}\frac{k_B T}{G^\eta} \tag{29}$$

Within the above assumptions, the main one being $D_A^\beta \ll D_B^\eta$ (i.e. β is indeed a barrier), the diffusivity through the barrier can be estimated by the experimental determination of thickness of η and the atomic fraction of A in the barrier. Alternatively, the approach in Eq. 25 can be used directly through a depth profile. This method can be advantageous over the method described in Sec. 4.1 if interfaces are not flat and/or the thickness of the growing phase η is not easily determined. It is in particular useful for techniques with high chemical sensitivity like secondary ion mass spectroscopy, APT or EDS-STEM. On the other hand, the approach of Sec. 4.1 (Eq. 17) allows to determine the kinetics of the growing phase for non-isothermal heat treatment and/or for intermediate cases when the diffusivity in the barrier and in the growing phase are similar. This approach should also allow to interpret in-situ measurements such as in-situ X-ray diffraction.

Finally, a similar approach can be used to determine the diffusion coefficient of B through the barrier using the growth of the phase δ.

$$D_B^\beta \quad = \quad \frac{1}{\Delta t}\frac{L^\beta}{c_B^\beta}\frac{k_B T}{\Delta\mu_B^\beta}\left(\int_\alpha c_B^\alpha dz + \int_\delta c_B^\delta dz\right) \tag{30}$$

where $\Delta\mu_B^\beta = \dfrac{G^\delta}{x_B^\delta}$.

4.3. Determination of Co and Si diffusivity through the Ti interlayer

Fig. 5 shows the diffusivity of Co in the Ti diffusion barrier determined from Eq. 29. These were obtained using the atomic fraction of Co in the Ti interlayer and the thickness of the growing CoSi layer corresponding to each annealing temperature. The Gibbs formation energy of CoSi, G^{CoSi}, was taken as $-50\mathrm{kJ/at\,g}$ [43], x_A^η as 0.5, and the atomic volumes of Ti and CoSi as $1.7 \cdot 10^{-29}\mathrm{m}^3$ and $1.1 \cdot 10^{-29}\mathrm{m}^3$. In Fig. 5, the diffusivity of Si in CoSi [19] is also reported. It can be seen that the diffusion of Si in CoSi is much faster than the diffusion of Co in the Ti layer (by about 5 orders of magnitude). It was also shown that the diffusion of Si in CoSi is faster than the diffusion of Co in CoSi [19] and thus that the growth of CoSi occurs by diffusion of Si. The main assumption used to establish Eq. 29 (i.e. $D_A^\beta \ll D_B^\eta$) is thus fulfilled and the growth of the CoSi layer is thus limited by the diffusion of Co through the Ti interlayer that acts as a diffusion barrier for Co. The diffusivity of Co in the present Ti interlayer can thus be determined by Eq. 29 and the following expression is obtained (Fig. 5):

$$D_{Co}^\beta \quad = \quad 47 \cdot \exp(-3.4\,\mathrm{eV}/k_B T)[\mathrm{m}^2/\mathrm{s}] \tag{31}$$

This expression is valid within the other assumption taken to derive Eq. 29. One of them is a constant atomic fraction of Co in the barrier, but the APT analysis reveals a more complex behavior (Fig. 2 and 3) with slight changes with temperature. This variation of composition with temperature may affect the diffusion and its dependency with temperature.

As noted in the results, Si does not only react with Co at the Ti/CoSi interface to form CoSi, but it also diffuses through the Ti barrier to penetrate inside the Co layer. This Si diffusion through the Ti interlayer occurs in order to form a solid solution in the Co phase and/or to segregate at Co grain boundaries as demonstrated in Fig. 3c. Co is stable either in a hexagonal phase (α-Co, room temperature) or a cubic phase (ϵ-Co, $T > 410\,^\circ\mathrm{C}$) [44]. In both Co phases, Si is reported to be soluble in equilibrium up to approximately $7\,\mathrm{at\,\%}$ at $T = 550\,^\circ\mathrm{C}$ and a relatively large amount of Si can thus be incorporated by diffusion at such a temperature. This diffusion configuration is described in Sec. 4.2 and the diffusivity of Si in the Ti interlayer

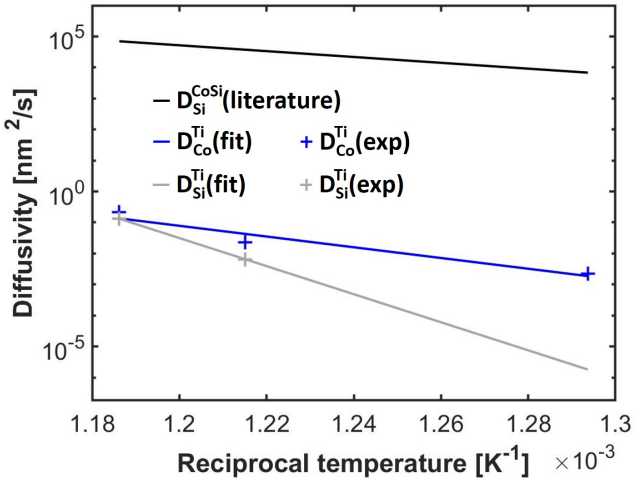

Figure 5: Arrhenius plot for the diffusion coefficient of Si in CoSi (black) [8], of Co in the Ti barrier (blue) determined by Eq. 21 and of Si in the Ti barrier (gray) determined by Eq. 26 and by Eq. 30 (cross = experiment, line = fit).

can be determined by Eq. 26. The integration was done using the concentration profile at 550 °C shown in Fig. 3b. This value is plotted in Fig. 5 together with the one at 570 °C determined by Eq. 30 taking into account the EDS profiles with a 50 nm Co_2Si layer (Fig. 1h). An average atomic fraction of 10 at % was taken for the barrier. From these 2 values, a very rough estimation of the temperature dependency can be done, but gives a very high activation energy (9 eV) and a pre-exponential factor ($6.6 \cdot 10^{34} m^2/s$) that is not realistic. The main cause for these unrealistic values can be that the diffusion of Si is not limited by the diffusion through the barrier, but by the diffusion in the Co layer. Indeed, for a transport limited by diffusion through the barrier, one may expect a flat concentration of Si in the Co layer, but the experimental profile of Si in Co (Fig. 3b) is typical for diffusion. The diffusivity of Si in the barrier at 550 °C should thus be higher than the one determined by Eq. 26 that is only a minimal value. A higher value at 550 °C will decrease the activation energy and the pre-exponential factor. Similarly, the diffusivity at 570 °C may be underestimated since all the Co top layer has been transformed in Co_2Si. This full transformation may have occurred before the end of heat treatment and the diffusivity at 570 °C obtained by Eq. 30 should be, once again, a minimal value. The two Si diffusivity in the interlayer are thus only indicative.

However, the Si diffusivity in the Ti interlayer appears to be lower than the

determined Co diffusivity in the Ti interlayer and both of them are much lower than the reported Si diffusivity in the growing CoSi phase [19]. It is unclear if the Si diffusivity in the barrier may become larger than the Co diffusivity at higher temperature, as suggested in Fig. 5. Indeed, even if the values in Fig. 5 are uncertain, there is no solution of Si in Co at 500 °C and CoSi forms first at the Ti/Si interface after Co diffuses through the entire Ti interlayer. This suggests that the activation energy for Si diffusivity in the barrier is indeed larger than the Co one.

Solution of Co in the Si substrate is also not measured in agreement with the very low (less than detection limit of APT) Co solubility in Si [45]. These conditions are thus following the assumptions for Eq. 26, at least at 500 °C, and that the determination of the Co diffusivity is the most accurate at 500 °C. For larger temperature, some Si diffuses through the barrier and Eq. 26 becomes less accurate. Nevertheless, it may be still considered as a good approximation.

It is observed that CoSi is formed on the Si side of the interlayer while the formation of Co_2Si occurs on the Co side of the interlayer. This can be understood if the nucleation of the two phases are considered. Indeed, as Co is diffusing faster than Si in the interlayer and as the solubility of Co in Si is very low, the solubility of Co in Si can be exceeded relatively fast leading to a supersaturation of Co in Si and thus creating the conditions for the nucleation of a Si rich phase. In principle, $CoSi_2$ has a larger driving force than CoSi and should also form low energy interface with Si since $CoSi_2$ and Si have similar structure. However, faster growth kinetics of CoSi than $CoSi_2$ may explain the observed formation of CoSi instead of $CoSi_2$.

On the contrary, the Si diffusion through the barrier can lead to supersaturation of the Co phase and finally to the nucleation of Co_2Si. Since the growth kinetics of Co_2Si is faster, this phase will grow. However, Co_2Si is formed in the Co layer on top of the Ti interlayer not before annealing at $T = 570\,°C$ for 10 min (Fig. 1d and Fig. 1h) due to the low Si diffusivity in the Ti interlayer.

Si is found inside the Co after diffusing through the Ti interlayer and segregates at Co grain boundaries at local atomic fractions up to 17 at %. This value exceeds the reported solubility of Si in Co that does not take into account grain boundary segregation. The very inhomogeneous distribution of Si in the Co layer before cobalt

silicide formation demonstrates the importance of a technique such as APT which considers any local concentration inhomogeneity in the volume in order to use the model of diffusion through a diffusion barrier driven by segregation or the formation of a solid solution (Sec. 4.2).

However, the presented simple models include several approximations which have to be printed out. For example, the measured thickness of the growing CoSi for each annealing step is taken as an average while the CoSi/Si interface is not flat and thereby the thickness varies (Fig. 1a-1d). In addition, the value of the CoSi Gibbs formation energy is taken from the Co-Si binary system [43]. Indeed, possible change in the Gibbs energy due to the presence of Ti is not considered. Furthermore, the determined Co and Si diffusivity in the Ti interlayer correspond to average values for the present Ti interlayer. (S)TEM (Fig. 1) and APT (Fig. 2 and Fig. 3) investigations show that the Ti interlayer is neither a single crystal layer nor purely Ti. Instead, the presence of carbon and oxygen indicates a TiC_x phase and oxide precipitates or a bilayer of TiC_x/TiC_xO_y. The determined diffusivities are representative for the Ti interlayer with its specific composition and microstructure including present phases, grain sizes, texture and possible precipitates. Even if no major changes were experimentally observed in our work, it is also possible that the properties of the barrier (composition, thickness, microstructure...) change during the heat treatments this will affect the diffusivities.

Finally, a steady state between the flux of Si through CoSi and the flux of Co through the Ti interlayer is assumed for the models in the presence of a diffusion barrier, but more complex behavior can be present. Furthermore, it is assumed that only one phase is growing in the model for reactive diffusion, but this is not the case at least at 550 °C and 570 °C. More complex models should be developed to better describe the growth of two phases (or one phase and a solid solution) on each side of the barrier).

Nevertheless, our simple models provide possibilities to determine and compare the permeability of interlayers for elements when reactive diffusion, or only diffusion takes place. Predictions of phase growth by reactive diffusion in the presence of a diffusion barrier can also be done if the diffusivity of reacting elements is known. In particular, the model of reactive diffusion in the presence of a diffusion barrier is

completing the model developed by Mangelinck et al. [11]. Their model describes the slowdown of the reactive diffusion growth by limiting the diffusion of the main diffusing species with an appropriate interlayer. The same effect is described in our model, but for another situation. We consider the case when the diffusion controlled growth is no more limited by the diffusion of the main diffusing species in the growing phase, but by the diffusion through the interlayer of the other reacting element which is separated from the reacting interface by the interlayer in which its permeability is low.

4.4. Ti segregation at the CoSi/Si interface

In Fig. 3, Ti is noted to diffuse towards the Si substrate after initial CoSi formation and to segregate at the CoSi/Si interface. This was predicted in the literature by Detavernier et al. [41]. They showed that a Ti capping layer affects $CoSi_2$ formation similarly to a Ti interlayer and explained their observations by a diffusion of Ti to the CoSi/Si interface. Our results give experimental evidence that Ti segregates at the CoSi/Si interface. This could affect the formation of $CoSi_2$ at higher annealing temperatures.

A similar result has been shown by Alberti et al. [46] who used energy filtered TEM imaging. Our APT result gives 3D information at atomic scale which are very useful for quantification of the Ti segregation [47, 48]. However, a single measurement with a single technique is limited in informative content due to a lack of crystallography information on the interface and statistics in view of experimental parameters (APT acquisition). This motivates for a systematic study on Ti segregation by selecting specific CoSi/Si interfaces and analyzing them with techniques such as TEM and APT which is not provided within this work.

5. Conclusion

A Co(100 nm)/Ti(5 nm)/Si(111) configuration was used to investigate the effect of a Ti interlayer on diffusion, phase formation and growth (reactive diffusion) at various annealing temperatures using (S)TEM imaging and EDS analysis in cross section as well as APT analysis. The Ti interlayer does not show significant changes in microstructure or composition for thermal annealing up to 570 °C. It acts as

a diffusion barrier between the Co layer and the Si substrate and retards reaction of both elements due to limited Co and Si permeability through the barrier. CoSi is the first formed silicide after annealing at 500 °C. It nucleates at the Ti/Si interface. Its growth is controlled by Co diffusion through the Ti interlayer. A model is developed for the reactive diffusion of a layer in the presence of a diffusion barrier when the growth rate is controlled by transport through the diffusion barrier of an element which is not the main diffusing species in the growing phase. Using this model, a Co diffusivity inside the Ti interlayer is found to be $D_{Co}^{Ti} = 1100 \cdot \exp(-3.4\,\mathrm{eV}/k_B T)$ [m^2/s]. Another model is developed using an estimated or measured number of atoms passing through the diffusion barrier and was used to estimate the diffusivity of Co or Si in the barrier. More generally, the presented models allow to determine elemental permeability in interlayers for material systems in which a phase is growing by reactive diffusion, or in which diffusion is occurring through the barrier due to segregation or the formation of a solid solution. This opens new ways to measure diffusion in very thin films.

In addition to the Co diffusion through the Ti interlayer towards the Si substrate, Si diffusion through the growing CoSi and the Ti interlayer towards the Co layer is observed and estimated with the developed model based on the integration of the depth profile. After segregation at Co grain boundaries with concentrations that exceed the solubility limit of Si in Co, Co_2Si is formed in the Co layer during annealing at 570 °C.

Finally, Ti is found to segregate at the CoSi/Si interface in accordance with prediction from literature. The segregated Ti is expected to influence $CoSi_2$ phase formation which takes place at higher annealing temperatures. Our result motivates for a systematic study of both, the Ti segregation at CoSi/Si interfaces related to the crystallography of the interface as well as a local study of the influence of the segregated Ti in the $CoSi_2$ phase formation.

Acknowledgments

This work was supported by the French government through the program "Investissements d'Avenir A*MIDEX" (Project APODISE, no. ANR-11-IDEX-0001-02) managed by the National Agency for Research (ANR). The authors would like

to thank Maxime Bertoglio, Marion Descoins of IM2NP and Andrea P. C. Campos and Martiane Cabie from the CP2M for discussions and technical assistance.

References

[1] S. P. Murarka, *Silicide thin films and their applications in microelectronics.* Intermetallics **3** (1995) 173–186.

[2] J. M. Poate, K. N. Tu, and J. W. Mayer, *Thin films: interdiffusion and reactions*, first ed. Wiley, New York, 1978.

[3] M.-A. Nicolet, and S. S. Lau, *Formation and Characterization of Transition-Metal Silicides.* VLSI Electronics Microstructure Science **6** (1983) 329–464.

[4] F. M. D'Heurle, and P. Gas, *Kinetics of formation of silicides: A review.* Journal of Materials Research **1** (1986) 205–221.

[5] M. Kajihara, *Analysis of kinetics of reactive diffusion in a hypothetical binary system.* Acta Materialia **52** (2004) 1193–1200.

[6] B. E. Deal, and A. S. Grove, *General relationship for the thermal oxidation of silicon.* Journal of Applied Physics **36** (1965) 3770–3778.

[7] D. Mangelinck. The growth of silicides and germanides. in: A. Paul, and S. Divinski (Eds.), *Handbook of Solid State Diffusion*, chapter 9, 379–446. Elsevier, Amsterdam, 2017.

[8] P. Gas, and F. M. D'Heurle, *Formation of silicide thin films by solid state reaction.* Applied Surface Science C **73** (1993) 153–161.

[9] A. E. Kaloyeros, and E. Eisenbraun, *Ultrathin diffusion barriers/liners for gigascale copper metallization.* Annu. Rev. Mater. Sci. **30** (2000) 363–385.

[10] T. Barge, P. Gas, and F. M. Dheurle, *Analysis of the Diffusion-Controlled Growth of Cobalt Silicides in Bulk and Thin-Film Couples.* Journal of Materials Research **10** (1995) 1134–1145.

[11] D. Mangelinck, T. Luo, and C. Girardeaux, *Reactive diffusion in the presence of a diffusion barrier: Experiment and model.* Journal of Applied Physics **123** (2018) 185301–(1–8).

[12] C. Detavernier, R. L. V. Meirhaeghe, F. Cardon, K. Maex, H. Bender, and S. Zhu, *CoSi2 formation in the Ti/Co/SiO2/Si system.* Journal of Applied Physics **88** (2000) 133–140.

[13] C. Detavernier, C. Lavoie, F. M. D'Heurle, H. Bender, and R. L. V. Meirhaeghe, *Low-temperature formation of CoSi2 in the presence of Au.* Journal of Applied Physics **95** (2004) 5340–5346.

[14] R. W. Cahn, and P. Haasen (Eds.), *Physical Metallurgy - vol 2*, fourth ed. North Holland, Amsterdam, 1996.

[15] L. M. Zhao, and Z. D. Zhang, *Effect of Zn alloy interlayer on interface microstructure and strength of diffusion-bonded Mg-Al joints.* Physical Metallurgy **58** (2008) 283–286.

[16] M. Bai, H. Jiang, Y. Chen, Y. Chen, C. Grovenor, X. Zhao, and P. Xiao, *Migration of sulphur in thermal barrier coatings during heat treatment.* Materials and Design **97** (2016) 364–371.

[17] Z. Zhang, B. Bai, H. Peng, S. Gong, and H. Guo, *Effect of Ru on interdiffusion dynamics of β-NiAl/DD6 system: A combined experimental and first-principles studies.* Materials and Design **88** (2015) 667–674.

[18] S. S. Lau, J. W. Mayer, and K. N. Tu, *Interactions in the Co/Si thin film system. I. Kinetics.* Journal of Applied Physics **49** (1978) 4005–4010.

[19] F. M. D'Heurle, and C. S. Petersson, *Formation of thin films of CoSi2: Nucleation and diffusion mechanisms.* Thin Solid Films **128** (1985) 283–297.

[20] J. C. Bean, and J. M. Poate, *Silicon/metal silicide heterostructures grown by molecular beam epitaxy.* Applied Physics Letters **37** (1980) 643–646.

[21] R. T. Tung, J. C. Bean, J. M. Gibson, J. M. Poate, and D. C. Jacobson, *Growth of single crystal CoSi2 on Si(111).* Applied Physics Letters **40** (1982) 684–686.

[22] K. De Keyser, C. Detavernier, J. Jordan-Sweet, and C. Lavoie, *Texture of CoSi2 films on Si(111), (110) and (001) substrates.* Thin Solid Films **519** (2010) 1277–1284.

[23] C.-S. Wei, D. B. Fraser, M. L. A. Dass, and T. Brat, *Formation of self-aligned TiN/CoSi2 bilayer from Co/Ti/Si and its applications in SALICIDE, diffusion barrier and contact fill.* VMIC Conference (1990) 233–239.

[24] M. L. A. Dass, D. B. Fraser, and C.-S. Wei, *Growth of epitaxial CoSi2 on (100)Si.* Applied Physics Letters **58** (1991) 1308–1311.

[25] K. Barmak, L. A. Clevenger, P. D. Agnello, E. Ganin, M. Copel, P. Dehaven, J. Falta, F. M. D'Heurle, and C. Cabrai, *Effect of an Interfacial Ti Layer on the Formation of CoSi2 on Si.* Mat. Res. Soc. Symp. Proc. **238** (1992).

[26] D. Kim, and H. Jeon, *Growth of CoSi2 using a Co/Zr bilayer on different Si substrates.* Thin Solid Films **346** (1999) 244–250.

[27] C. Detavernier, R. L. Van Meirhaeghe, F. Cardon, K. Maex, H. Bender, B. Brijs, and W. Vandervorst, *Formation of epitaxial CoSi2 by a Cr or Mo interlayer: Comparison with a Ti interlayer.* Journal of Applied Physics **89** (2001) 2146–2150.

[28] C. Detavernier, C. Lavoie, and R. L. Van Meirhaeghe, *CoSi2 formation in the presence of Ti, Ta or W.* Thin Solid Films **468** (2004) 174–182.

[29] H. B. R. Lee, J. Y. Son, and H. Kim, *Nitride mediated epitaxy of Co Si2 through self-interlayer-formation of plasma-enhanced atomic layer deposition Co.* Applied Physics Letters **90** (2007) 2005–2008.

[30] R. T. Tung, *Oxide mediated epitaxy of CoSi2 on silicon.* Applied Physics Letters **68** (1996) 3461.

[31] T. G. Finstad, *A Xe marker study of the transformation of Ni2Si to NiSi in thin films.* Physica Status Solidi (a) **63** (1981) 223–228.

[32] D. B. William, and C. B. Carter, *Transmission Electron Microscopy*, second ed. Springer, New York, 2009.

[33] B. Gault, M. P. Moody, J. M. Cairney, and S. P. Ringer, *Atom Probe Microscopy*, first ed. Springer, New York, 2012.

[34] W. Lefebvre, F. Vurpillot, and X. Sauvage, *Atom Probe Tomography: Put Theory Into Practice*, first ed. Academic Press, Elsevier Science, 2016.

[35] J. Mayer, L. A. Giannuzzi, T. Kamino, and J. Michael, *TEM Sample Preparation and Damage*. MRS Bulletin **32** (2007) 400–407.

[36] M. K. Miller, K. F. Russell, K. Thompson, R. Alvis, and D. J. Larson, *Review of Atom Probe FIB-Based Specimen Preparation Methods*. Microscopy and Microanalysis **13** (2007) 428–436.

[37] P. Bas, A. Bostel, B. Deconihout, and D. Blavette, *A general protocol for the reconstruction of 3D atom probe data*. Applied Surface Science **87-88** (1995) 298–304.

[38] F. Vurpillot, B. Gault, B. P. Geiser, and D. J. Larson, *Reconstructing atom probe data: A review*. Ultramicroscopy **132** (2013) 19–30.

[39] P. J. Warren, A. Cerezo, and G. D. W. Smith, *Observation of atomic planes in 3DAP analysis*. Ultramicroscopy **73** (1998) 261–266.

[40] O. C. Hellman, J. A. Vandenbroucke, J. Rüsing, D. Isheim, and D. N. Seidman, *Analysis of Three-dimensional Atom-probe Data by the Proximity Histogram*. Microscopy and Microanalysis **6** (2000) 437–444.

[41] C. Detavernier, R. L. Van Meirhaeghe, F. Cardon, K. Maex, W. Vandervorst, and B. Brijs, *Influence of Ti on CoSi2 nucleation*. Applied Physics Letters **77** (2000) 3170–3172.

[42] M. J. H. Van Dal, D. G. G. M. Huibers, A. A. Kodentsov, and F. J. J. Van Loo, *Formation of Co-Si intermetallics in bulk diffusion couples. Part I. Growth kinetics and mobilities of species in the silicide phases*. Intermetallics **9** (2001) 409–421.

[43] M. E. Schlesinger, *Thermodynamics of Solid Transition-Metal Silicides*. Chemical Reviews **90** (1990) 607–628.

[44] O. Bodak, and N. Lebrun. Cobalt – silicon – titanium. in: G. Effenberg, and S. Ilyenko (Eds.), *Ternary Alloy Systems: Phase Diagrams, Crystallographic and Thermodynamic Data critically evaluated by MSIT. Light Metal Systems. Part 4*, 178–184. Springer, Berlin Heidelberg, 2006.

[45] T. B. Massalski, J. L. Murray, L. H. Bennett, and H. Baker, *Binary alloy phase diagrams*, first ed. ASM International, 1986.

[46] A. Alberti, R. Fronterrè, F. La Via, and E. Rimini, *Effect of a Ti Cap Layer on the Diffusion of Co Atoms during CoSi2 Reaction.* Electrochemical and Solid-State Letters **8** (2005) G47.

[47] B. W. Krakauer, and D. N. Seidman, *Absolute atomic-scale measurements of the Gibbsian interfacial excess of solute at internal interfaces.* Physical Review B **48** (1993) 6724–6727.

[48] Z. Peng, Y. Lu, C. Hatzoglou, A. Kwiatkowski Da Silva, F. Vurpillot, D. Ponge, D. Raabe, and B. Gault, *An Automated Computational Approach for Complete In-Plane Compositional Interface Analysis by Atom Probe Tomography.* Microscopy and Microanalysis **25** (2019) 389–400.